Do we need demographic data to forecast population responses to climate change?

Andrew T. Tredennick[*1], Peter B. Adler[1], and Mevin B. Hooten[2,3,4]

[1]*Department of Wildland Resources and the Ecology Center, 5230 Old Main Hill, Utah State University, Logan, Utah 84322 USA*

[2]*U.S. Geological Survey, Colorado Cooperative Fish and Wildlife Research Unit, Colorado State University, Fort Collins, CO 80523 USA*

[3]*Department of Fish, Wildlife, and Conservation Biology, Colorado State University, Fort Collins, CO 80523 USA*

[4]*Department of Statistics, Colorado State University, Fort Collins, CO 80523 USA*

Abstract. Rapid climate change has generated growing interest in forecasts of future population trajectories. Traditional population models, typically built using detailed demographic observations from one study site, can address climate change impacts at one location, but are difficult to scale up to the landscape and regional scales relevant to management decisions. An alternative is to build models using population-level data that are much easier to collect over broad spatial scales than individual-level data. However, such models ignore the fact that climate drives population growth through its influence on individual performance. Here, we test the consequences of aggregating individual responses when forecasting climate change impacts on four perennial grass species in a semi-arid grassland in Montana, USA. We parameterized two population models for each species, one based on individual-level data (survival, growth and recruitment) and one on population-level data (percent cover), and compared their accuracy, precision, and sensitivity to climate variables.

*Corresponding author: atredenn@gmail.com

For both models we used Bayesian ridge regression to identify the optimal predictive model in terms of climate covariate strengths. The individual-level model was more accurate and precise than the aggregated model when predicting out-of-sample observations. When comparing climate effects from both models, the population-level model missed important climate effects from at least one vital rate for each species. Increasing the sample size at the population-level would not necessarily reduce forecast uncertainty; the way to reduce uncertainty is to capture unique climate dependence of individual vital rates. Our analysis indicates that there is no shortcut to forecasting climate change impacts on plant populations — detailed demographic data are essential. Despite the superiority of the individual-level model, the forecasts it generated still were too uncertain to be useful for decision-makers. We need new methods to collect demographic data efficiently across environmental gradients in space and time.

Key words: forecasting, climate change, grassland, integral projection model, population model

Introduction

Perhaps the greatest challenge for ecology in the 21st century is to forecast the impacts of environmental change (Clark et al. 2001, Petchey et al. 2015). Forecasts require sophisticated modeling approaches that fully account for uncertainty and variability in both ecological process and model parameters (Luo et al. 2011, but see Perretti et al. 2013 for an argument against modeling the ecological process). The increasing statistical sophistication of population models (Rees and Ellner 2009) makes them promising tools for predicting the impacts of environmental change on species persistence and abundance. But reconciling the scales at which population models are parameterized and the scales at which environmental changes play out remains a challenge (Clark et al. 2010, 2012, Freckleton et al. 2011, Queenborough et al. 2011). The problem is that most population models

are built using data from a single study site because collecting those data, which involves tracking the fates of individuals plants, is so difficult. The resulting models cannot be applied to the landscape and regional scales relevant to decision-making without information about how the fitted parameters respond to spatial variation in biotic and abiotic drivers (Sæther et al. 2007). The limited spatial extent of individual-level demographic datasets constrains our ability to use population models to address applied questions about the consequences of climate change.

The inability of most population models to address landscape-scale problems may explain why land managers and conservation planners have embraced species distribution models (SDMs) (see Guisan and Thuiller 2005 for a review). SDMs typically rely on easy-to-collect presence/absence data (but see Clark et al. 2014 for new methods) and remotely-sensed environmental covariates that allow researchers to model large spatial extents (e.g., Maiorano et al. 2013). Thus, it is relatively straightforward to parameterize and project SDMs over landscapes and regions. However, the limitations of SDMs are well known (Pearson and Dawson 2003, Elith and Leathwick 2009, Araújo and Peterson 2012). Ideally, researchers would provide managers with landscape-scale population models, combining the extent of SDMs with information about dynamics and species abundances (Schurr et al. 2012, Merow et al. 2014).

Aggregate measures of population status, rather than individual performance, offer an intriguing alternative for modeling populations (Clark and Bjørnstad 2004, Freckleton et al. 2011). Population-level data cannot provide inference about demographic mechanisms, but might be sufficient for modeling future population states, especially since such data are feasible to collect across broad spatial extents (e.g., Queenborough et al. 2011). The choice between individual and population-level data involves a difficult trade-off: while individual-level data leads to more mechanistic models, population-level data leads to models that can be applied over greater spatial and temporal extents. An open question is how much forecasting skill is lost when we build models based on population rather than

individual-level data.

To date, most empirical population modelers have relied on individual-level data, with few attempts to capitalize on population-level measures. An important exception was an effort by Taylor and Hastings (2004) to model the population growth rate of an invasive species to identify the best strategies for invasion control. They used a "density-structured" model where the state variable is a discrete density state rather than a continuous density measure. Such models do not require individual-level demographic data and can adequately describe population dynamics. Building on Taylor and Hastings (2004), Freckleton et al. (2011) showed that density-structured models compare well to continuous models in theory, and Queenborough et al. (2011) provide empirical evidence that density-structured models are capable of reproducing population dynamics at landscape spatial scales, even if some precision is lost when compared to fully continuous models. The appeal of density-structured approaches is clear. However, none of these models included environmental covariates.

Addressing climate change questions with models fit to population-level data is potentially problematic. It is individuals, not populations, that respond to climate variables (Clark et al. 2012). Ignoring this fact amounts to an "ecological fallacy", where inference about the individual relies on statistical inference on the group (Piantadosi et al. 1988). Population growth (or decline) is the outcome of demographic processes such as survival, growth, and recruitment that occur at the level of individual plants. Climate can affect each demographic process in unique, potentially opossing, ways (Dalgleish et al. 2011). These unique climate responses may be difficult to resolve in statistical models based on population-level data where demographic processes are not identifiable. If important climate effects are missed because of the aggregation inherent in in population-level data, then population models built with such data will make uninformative or unreliable forecasts.

Here, we compare the forecasting skill of statistical and population models based on aggre-

4

gated, population-level data with models based on individual-level data. We used a unique demographic dataset that tracks the fates of individual plants from four species over 14 years to build two kinds of single-species population models, traditional models using individual growth, survival, and recruitment data and alternative models based on basal cover. In both models, interannual variation is explained, in part, by climate covariates. We first quantify forecasting skill using cross-validation. We then performed simulations to quantify the sensitivies of species' cover to small perturbations in average precipitation and temperature. Based on the cross-validation results, predictions of individual level models were clearly better, but, unfortunately, still too uncertain to inform management decisions.

Materials and Methods

Study site and data

Our demographic data come from the Fort Keogh Livestock and Range Research Laboratory in eastern Montana's northern mixed prairie near Miles City, Montana, USA (46° 19' N, 105° 48' W). The dataset is freely available on Ecological Archives[1] (Anderson et al. 2011), and interested readers should refer to the metadata for a complete description. The site is about 800 m above sea level and mean annual precipitation (1878-2009) is 334 mm, with most annual precipitation falling from April through September. The community is grass-dominated, and we focused on the four most abundant grass species: *Bouteloua gracilis* (BOGR), *Hesperostipa comata* (HECO), *Pascopyrum smithii* (PASM), and *Poa secunda* (POSE) (Fig. 1). *B. gracilis* is a warm-season perennial grass, whereas *H. comata*, *P. smithii*, and *P. secunda* are cool-season perennial grasses. All species typically begin growth in the early spring, reach maximum growth and flower in early to mid summer (May-June), and disperse seed in mid to late summer (July-September).

From 1932 to 1945 individual plants were identified and mapped annually in 44 1-m^2

---

[1]http://esapubs.org/archive/ecol/E092/143/

quadrats using a pantograph. The quadrats were distributed in six pastures, each as-signed a grazing treatment of light (1.24 ha/animal unit month), moderate (0.92 ha/aum), and heavy (0.76 ha/aum) stocking rates (two pastures per treatment). In this analysis we account for potential differences among the grazing treatments, but do not focus on grazing×climate interactions. The annual maps of the quadrats were digitized and the fates of individual plants tracked and extracted using a computer program (Lauenroth and Adler 2008, Chu et al. 2014). The permanent quadrats have not been relocated, but their distribution in six different pastures means the data represent a broad spatial distribution for the study area. Daily climate data are available for the duration of the data collection period (1932 - 1945) from the Miles City airport, Wiley Field, 9 km from the study site.

We modeled each grass population based on two levels of data: individual and quadrat (Fig. 2). The individual data is the "raw" data. For the quadrat-level we data we simply sum individual basal cover for each quadrat by species. This is equivalent to a near-perfect census of quadrat percent cover because previous analysis shows that measurement error at the individual-level is small (Chu and Adler 2014). Based on these two datasets we can compare population models built using individual-level data and aggregated, quadrat-level data. At the individual level we explicitly model three vital rates: growth (13 year-to-year transitions, 29 quadrats, 18,730 records), survival (13 years, 33 quadrats, 29,353 records), and recruitment (13 years, 33 quadrats, 304 records). At the quadrat level we model popu-lation growth as change in percent cover of quadrats with non-zero cover in year t and in year t-1 (13 year-to-year transitions, 29 quadrats, 866 records). For modeling population growth at the quadrat level we ignore within-quadrat extirpation and colonization events because they are very rare in our time series ($N = 16$ and $N = 13$, respectively, across all species). Given the broad spatial distribution of the quadrats we are studying, it is safe to assume that these events are in fact rare enough to be ignored for our purposes.

All R code and data necessary to reproduce our analysis is archived on GitHub as release

v1.0[2] (http://github.com/atredennick/MicroMesoForecast/releases). That stable release will remain static as a record of this analysis, but subsequent versions may appear if we update this work. We have also deposited the v1.0 release on Dryad (*link here after acceptance*).

Stastical models of vital rates

At both levels of inference (individual and quadrat), the building blocks of our population models are vital rate regressions. For individual-level data, we fit regressions for survival, growth, and recruitment for each species. At the quadrat-level, we fit a single regression model for population growth. We describe the statistical models separately since fitting the models required different approaches. All models contain five climate covariates that we chose *a priori*: "water year" precipitation at *t*-2 (lagppt); April through June precipitation at *t*-1 and *t* (ppt1 and ppt2, respectively) and April through June temperature at *t*-1 and *t* (TmeanSpr1 and TmeanSpr2, respectively), where *t*-1 to *t* is the transition of interest. We also include interactions among same-year climate covariates (e.g., ppt1 × TmeansSpr1).

We fit all models using a hierarchical Bayesian approach. The models are fully descibed in Appendix A, so here we focus on the main process and the model likelihood. For the likelihood models, $\mathbf{y}^X$ is always the relevant vector of observations for vital rate X ($X = S$, G, R, or P) for survival, growth, recruitment, or population growth). For example, $\mathbf{y}^S$ is a vector of 0's and 1's indicating whether a genet survives from *t* to *t+1*, or not. All model parameters are species-specific, but we omit subscripts for species in model descriptions below to reduce visual clutter.

---

[2] *Note to reviewers*: so that v1.0 will be associated with the published version of the manuscript, we have released v0.1 to be associated with this review version.

7

Vital rate models at the individual level We used logistic regression to model survival probability (s) of a genet:

$$\mathbf{y}^S \sim \text{Bernoulli}(\mathbf{s}) \tag{1}$$

$$\text{logit}[s(x, \mathbf{z}_t, w)] = \beta_{0,t} + \beta_{s,t}x + \beta_Q + \mathbf{z}_t'\boldsymbol{\beta}_c + \beta_{d,1}w + \beta_{d,2}(xw) \tag{2}$$

where x is the log of genet basal area, $\beta_{0,t}$ is a year specific intercept intercept, β_Q is the random effect of quadrat group location, $\beta_{s,t}$ is the year-specific slope parameter for size, $\mathbf{z}$ is a vector of i climate covariates specific to year t, $\boldsymbol{\beta}_c$ is a vector of fixed climate effects of length i, $\beta_{d,1}$ is the effect of intraspecific crowding experienced by the focal genet (w), and $\beta_{d,2}$ is a size by crowding (xw) interaction effect.

We modeled growth as a Gaussian process describing genet size at time $t + 1$ as a function of size at t and climate covariates:

$$\mathbf{y}^G \sim \text{Normal}(\boldsymbol{\mu}, \sigma_{x,t}^2) \tag{3}$$

$$\mu(x, \mathbf{z}_t, w) = \beta_{0,t} + \beta_{s,t}x + \beta_Q + \mathbf{z}_t'\boldsymbol{\beta}_c + \beta_{d,1}w + \beta_{d,2}(xw) \tag{4}$$

where $\mu(x, \mathbf{z}_t, w)$ is log of predicted genet size at time $t + 1$, and all other parameters are as described for the survival regression. We capture non-constant error variance in growth by modeling the variance around the growth regression ($\sigma_{x,t}^2$) as a nonlinear function of predicted genet size:

$$\sigma_{x,t}^2 = a \exp[b \times \mu(x, \mathbf{z}_t, w)] \tag{5}$$

where $\mu(x, \mathbf{z}_t, w)$ is log of predicted genet size predicted from the growth regression (Eq. 4), and a and b are constants.

Our data allows us to track new recruits, but we cannot assign a specific parent to new genets. Therefore, we model recruitment at the quadrat level. We assume the number of individuals, y^R, recruiting at time $t + 1$ in quadrat q follows a negative binomial distribution:

8

$$y_{q,t+1}^R \sim \text{NegBin}(\lambda_{q,t+1}, \phi) \tag{6}$$

where λ is the mean intensity and ϕ is the size parameter. We define λ as a function of quadrat composition and climate in the previous year:

$$\lambda_{q,t+1} = C_{q,t}' \exp\left(\beta_{0,t} + \beta_Q + \mathbf{z}_t'\boldsymbol{\beta}_c + \beta_d\sqrt{C_{q,t}'}\right) \tag{7}$$

where C' is effective cover (cm^2) of the focal species in quadrat q, and all other terms are as in the survival and growth regressions. Effective cover is a mixture of observed cover (C) in the focal quadrat (q) and the mean cover across the entire group $(\bar{C})$ of Q quadrats in which q is located:

$$C_{q,t}' = pC_{q,t} + (1-p)\bar{C}_{Q,t} \tag{8}$$

where p is a mixing fraction between 0 and 1 that is estimated within the model.

Population model at the quadrat level The statistical approach used to model aggregated data depends on the type of data collected. We have percent cover data, which can easily be transformed to proportion data. An obvious choice for fitting a linear model to proportion data is beta regression because the support of the beta distribution is [0,1], not including true zeros or ones. However, when we used fitted model parameters from a beta regression in a quadrat-based population model, the simulated population tended toward 100% cover for all species. We therefore chose a modeling approach based on a truncated log-normal likelihood. The model for quadrat cover change from time t to $t+1$ is

$$\mathbf{y}^P \sim \text{LogNormal}(\mu(x, \mathbf{z}_t), \sigma^2)\text{T}[0,1] \tag{9}$$

$$\mu(x, \mathbf{z}_t) = \beta_{0,t} + \beta_{s,t}x + \beta_Q + \mathbf{z}_t'\boldsymbol{\beta}_c \tag{10}$$

9

where $\mu(x, \mathbf{z}_t)$ is the log of proportional cover in quadrat q at time $t + 1$, and all other parameters are as in the individual-level growth model (Eq. 4) except that x now represents log of proportional cover. The log normal likelihood includes a truncation (T[0,1]) to ensure that predicted values do not exceed 100% cover.

Model fitting and stastical regularization

Model fitting   Our Bayesian approach to fitting the vital rate models required choosing appropriate priors for unknown parameters and deciding which, if any, of those priors should be hierarchical. We decided to fit models where all terms were fit by species. Within a species, we fit yearly size effects and yearly intercepts hierarchically where year-specific coefficients were drawn from global distributions representing the mean size effect and intercept. Quadrat random effects were also fit hierarchically, with quadrat offsets being drawn from distributions with mean zero and a shared variance term (independent Gaussian priors, Appendix A). Climate effects were not modeled hierarchically, and each was given a diffuse prior distribution. We used standard diffuse priors for all unknown parameters (Appendix A).

All of our analyses (model fitting and simulating) were conducted in R (R Core Team 2013). We used the 'No-U-Turn' MCMC sampler in Stan (Stan Development Team 2014a) to estimate the posterior distributions of model parameters using the package 'rstan' (Stan Development Team 2014b). We obtained posterior distributions for all model parameters from three parallel MCMC chains run for 1,000 iterations after discarding an initial 1,000 iterations. Such short MCMC chains may surprise readers more familiar with other MCMC samplers (i.e. JAGS or WinBUGS), but the Stan sampler is exceptionally efficient, which reduces the number of iterations needed to achieve convergence. We assessed convergence visually and made sure scale reduction factors for all parameters were less than 1.01. For the purposes of including parameter uncertainty in our population models, we saved the final 1,000 iterations from each of the three MCMC chains to be used as ran-

10

₂₄₂ domly drawn values during population simulation. This step alleviates the need to reduce

₂₄₃ model parameters by model selection since sampling from the full parameter space in the

₂₄₄ MCMC ensures that if a parameter broadly overlaps zero, on average the effect in the pop-

₂₄₅ ulation models will also be near zero. We report the posterior mean, standard deviation,

₂₄₆ and 95% Bayesian Credible Intervals for every parameter of each model for each species in

₂₄₇ Appendix B.

₂₄₈ **Statistical regularization: Bayesian ridge regression**   Our objective is to model

₂₄₉ the response of our focal grass species to interannual variation in climate, even if those

₂₅₀ responses are weak. Therefore, we avoid selecting among models with all possible com-

₂₅₁ binations of climate covariates, and instead use Bayesian ridge regression to regulate, or

₂₅₂ constrain, the posterior distributions of each climate covariate (Hooten and Hobbs 2015).

₂₅₃ Ridge regression is a specific application of statistical regularization that seeks to opti-

₂₅₄ mize model generality by trading off bias and variance. As the name implies, statistical

₂₅₅ regularization involves the use of a regulator that constrains an optimization. The natural

₂₅₆ regulator in a Bayesian application is the prior on the coefficient of interest. Each of our

₂₅₇ statistical models includes the effects of climate covariates via the term $\mathbf{z}_t'\boldsymbol{\beta}_c$ with prior

₂₅₈ $\boldsymbol{\beta}_c \sim \text{Normal}(\boldsymbol{\mu}_{\beta_c}, \sigma^2_{\beta_c})$. Since we standardized all climate covariates to have mean zero

₂₅₉ and variance one, we can set $\boldsymbol{\mu}_{\beta_c} = 0$ and let $\sigma^2_{\beta_c}$ serve as the regulator that can shrink

₂₆₀ covariates toward zero – the smaller the prior variance, the more the posteriors of $\boldsymbol{\beta}_c$ are

₂₆₁ shrunk toward zero, and the stronger the penalty (Hooten and Hobbs 2015).

₂₆₂ To find the optimal penalty (i.e., optimal value of the hyperparameter $\sigma^2_{\beta_c}$), we fit each

₂₆₃ statistical model with a range of values for $\sigma^2_{\beta_c}$ and compared predictive scores from leave-

₂₆₄ one-year-out cross-validation. We performed the grid search over 24 values of $\sigma^2_{\beta_c}$, ranging

₂₆₅ from $\sigma^2_{\beta_c} = 0.01$ to $\sigma^2_{\beta_c} = 2.25$. For each statistical model and each species we fit $13 \times$

₂₆₆ $24 = 312$ models (13 years to leave out for cross-validation and 24 values of $\sigma^2_{\beta_c}$) – a total

₂₆₇ of 4,992 models. We calculated the log pointwise predictive density (*lppd*) to score each

model's ability to predict the left-out data. Thus, for training data y_{train} and held-out data y_{hold} at a given value of σ_θ^2 across all MCMC samples $s = 1, 2, ..., S$ and all hold outs of data from year t to year T, and letting θ represent all unknowns, *lppd* is

$$\text{lppd}_{\text{CV}} = \sum_{t=1}^{T} \log_e \int [y_{t,hold}|\theta][\theta|y_{train}]d\theta, \tag{11}$$

and computed as

$$\sum_{t=1}^{T} \log_e \left(\frac{1}{S} \sum_{s=1}^{S} (y_{t,hold}|\theta_{ts}) \right). \tag{12}$$

We chose the optimal prior variance for each species-statistical model combination as the one that produced the highest *lppd* and then fit each species-statistical model combination using the full data set for each species and the optimal prior variance.

Population models

With the posterior distribution of the vital rate statistical models in hand, it is straightforward to simulate the population models. We used an Integral Projection Model (IPM) to model populations based on individual-level data (Ellner and Rees 2006) and a quadrat-based version of an individually-based model (Quadrat-Based Model, QBM) to model populations based on quadrat-level data. We describe each in turn.

Integral projection model We use a stochastic IPM (Rees and Ellner 2009) that includes the climate covariates from the vital rate statistical models. In all simulations we ignore the random year effects so that interannual variation is driven solely by climate. We fit the random year effects in the vital rate regressions to avoid over-attributing variation to climate covariates. Our IPM follows the specification of Chu and Adler (2015) where the population of species j is a density function $n(u_j, t)$ giving the density of sized-u genets at time t. Genet size is on the natural log scale, so that $n(u_j, t)du$ is the number of genets

12

whose area (on the arithmetic scale) is between e^{u_j} and e^{u_j+du}. The density function for any size v at time $t+1$ is

$$n(v_j, t+1) = \int_{L_j}^{U_j} k_j(v_j, u_j, \bar{w}_j(u_j))n(u_j, t) \tag{13}$$

where $k_j(v_j, u_j, \bar{w}_j)$ is the population kernel that describes all possible transitions from size u to v and $\bar{w}_j$ is a scalar representing the average intraspecific crowding experienced by a genet of size u_j and species j. The integral is evaluated over all possible sizes between predefined lower (L) and upper (U) size limits that extend beyond the range of observed genet sizes.

Since the IPM is spatially-implicit, we cannot calculate neighborhood crowding for specific genets (w_{ij}). Instead, we use an approximation ($\bar{w}_j$) that captures the essential features of neighborhood interactions (Adler et al. 2010). This approximation relies on a 'no-overlap' rule for conspecific genets to approximate the overdispersion of large genets in space (Adler et al. 2010).

The population kernel is defined as the joint contributions of survival (S), growth (G), and recruitment (R):

$$k_j(v_j, u_j, \bar{w}_j) = S_j(u_j, \bar{w}_j(u_j))G_j(v_j, u_j, \bar{w}_j(u_j)) + R_j(v_j, u_j, \bar{w}_j), \tag{14}$$

which means we are calculating growth (G) for individuals that survive (S) from time t to $t+1$ and adding in newly recruited (R) individuals of an average sized one-year-old genet for the focal species. Our stastical model for recruitment (R, described above) returns the number of new recruit produced per quadrat. Following previous work (Adler et al. 2012, Chu and Adler 2015), we assume that fecundity increases linearly with size ($R_j(v_j, u_j, \bar{w}_j) = e^{u_j}R_j(v_j, \bar{w}_j)$) to incorporate the recruitment function in the spatially-implicit IPM.

We used random draws from the final 1,000 iterations from each of three MCMC chains

to introduce stochasticity into our population models. At each time step, we randomly selected climate covariates from one of the 14 observed years. Then, we drew the full parameter set (climate effects and density-dependence fixed effects) from a randomly selected MCMC iteration. Using this approach, rather than simply using coefficient point estimates, captures the effect of parameter uncertainty. Relatively unimportant climate covariates (those that broadly overlap 0) will have little effect on the mean of the simulation results, but can contribute to their variation. Since our focus was on the contribution of climate covariates to population states, we set the random year effects and the random group effects to zero.

Quad-based model To simulate our quad-based model (QBM), we simply iterate the quadrat-level statistical model (Eqs. 9-10). We use the same approach for drawing parameter values as described for the IPM. After drawing the appropriate parameter set, we calculate the mean response (log cover at $t+1 = \mu_{t+1}$) according to Eq. 10. We then make a random draw from a [0,1] truncated lognormal distribution with mean equal to μ_{t+1} from Eq. 10 and the variance estimate from the fitted model. We can then project the model forward by drawing a new parameter set (unique to climate year and MCMC iteration) at each timestep. As with the IPM, random year effects are ignored for all simulations.

Model validation

To test each model's ability to forecast population state, we made out-of-sample predictions using leave-one-year-out cross validation. For both levels of modeling, we fit the vital rate models using observations from all years except one, and then used those fitted parameters in the population models to perform a one-step-ahead forecast for the year whose observations were withheld from model fitting. Within each observation year, several quadrats were sampled. We made predictions for each observed quadrat in the focal year, initializing each simulation with cover in the quadrat the previous year. Since we

14

were making quadrat-specific predictions, we incorporated the group random effect on the intercept for both models. We repeated this procedure for all 13 observation years, making 100 one-step-ahead forecasts for each quadrat-year combination with parameter uncertainty included via random draw from the MCMC chain as described above. Random year effects were set to zero since year effects cannot be assigned to unobserved years.

This cross-validation procedure allowed us to compare accuracy and precision of the two modeling approaches (IPM versus QBM). We first calculated the median predicted cover across the 100 simulations for each quadrat-year and then calculated the absolute error as the absolute value of the difference between the observed cover for a given quadrat-year and the median prediction. To arrive at mean absolute error (MAE), we then averaged the absolute error within each species across the quadrat-year specific errors. We use MAE as our measure of accuracy. To measure precision we calculated the distance between the upper and lower 90th quantiles of the 100 predictions and averaged this value over quadrat-years for each species.

Testing sensitivity to climate covariates

With our fitted and validated models in hand, we ran simulations for each model type (IPM and QBM) under four climate perturbation scenarios: (1) observed climate, (2) precipitation increased by 1%, (3) temperature increased by 1%, and (4) precipitation and temperature increased by 1%. We ran the simulations for 2,500 time steps, enough to estimate equilibrium cover after discarding an initial 500 time steps as burn-in. Each simulation was run under two parameter scenarios: (1) using mean parameter estimates and (2) using randomly drawn parameters from the MCMC chain. We use (1) to detect the overall sensitivity of equilibrium cover to climate, and we use (2) to show the impact of model and parameter uncertainty on forecast precision.

As an effort to identify potential discrepencies between IPM and QBM forecasts, we also

ran simulations designed to quantify the sensitivities of individual and combined vital rates to climate for the IPM. Specifically, we ran simulations for the above climate scenarios, but applied the perturbed climate covariates to survival, growth, or recruitment vital rates individually and in pairwise combinations. This allowed us to isolate the vital rate(s) most sensitive to climate. For this analysis, we used mean parameter estimates to reduce the sources of uncertainty in the sensitivity estimates.

We expected the IPM to produce more accurate and precise forecasts due to either (1) the smaller sample size of the quadrat level data sets compared to the individual level data sets, leading to larger parameter uncertainty for the QBM, or (2) the QBM climate effects being weakly associated with one or more vital rate climate effects at the individual level. To assess the impact of sample size on QBM parameter uncertainty we refit the QBM statistical model (Eqs. 9-10) after removing sets of 2, 5, 10, and 15 quadrats. We fit 10 models at each level of quadrat removal (2, 5, 10, 15 quadrats), removing a different randomly selected set of quadrats for each fit. We calculated the standard deviation of climate main effects (pptLag, ppt1, ppt2, TmeanSpr1, and TmeanSpr2) for each model and averaged those over replicates within each set of quadrat removals. This allowed us to regress parameter uncertainty against sample size.

To deterime if the QBM climate effects are correlated with climate effects for each vital rate model in the IPM, we simply regressed the QBM climate coefficients against each vital rate model's climate coefficients and calculated Pearson's ρ. Strong correlations indicate the QBM is capable of detecting climate effects associated with individual vital rates. A weak correlation indicates the QBM "misses" the climate effect on a particular vital rate.

16

Results

Comparison of forecast models

Sensitivity of models to climate

The response of a population to climate change is a result of the aggregate effects of climate on individual vital rates. Since the IPM approach relies on vital rate regressions, we were able to quantify the sensitivity of each vital rate in isolation and in pairwise combinations. Across all species, climate covariates can have opposing effects on different vital rates (Fig. 3). Growth was the most sensitive vital rate for all species, showing a negative response to increased precipitation, and stronger positive response to increased temperature, and a mostly positive response when both climate factors are increased (Fig. 3). *B. gracilis* survival rates were sensitive to temperature, resulting in an increase in plant cover under increased temperature (Fig. 3a). In isolation, recruitment and survival were insensitive to climate factors for *H. comata* (Fig. 3b). Survival and recruitment of *P. smithii* were both sensitive, negatively, to temperature and precipitation (Fig. 3c). *P. secunda* equilibrium cover was sensitive to the climate effects on survival and recruitment, showing a negative effect on both vital rates for increased precipitation, but a strong positive effect on survival with increased temperature (Fig. 3d). Equilibrium cover responded negatively when increased precipitation and temperature affect recruitment (Fig. 3d). At least two of three vital rates were sensitive to climate for each species (Fig. 3).

Sources of uncertainty in the QBM

Sample size had a relatively weak effect on QBM climate parameter uncertainty after the number of quadrats used in fitting exceeded about 10 (Fig. 5). Inverse-gaussian fits show that increasing sample size beyond the number of quadrats we used would result in diminishing returns in terms of parameter certainty (Fig. 5).

17

Climate effects estimated from the QBM are most correlated with climate effects from the growth regression at the individual level (Fig. 6). In no case does the QBM statistical model have strong correlations across all three vital rates (Fig. 6). QBM climate effects were most weakly correlated with those from individual-level recruitment models for *B. gracilis*, *H. comata*, and *P. secunda* (Fig. 6a,b,d). For *P. smithii*, QBM climate effects showed no correlation with the survival model effects (Fig. 6c).

Model forecasts

Forecasts based on 1% climate changes were extremely uncertain when we considered model error and parameter uncertainty (Fig. 6; simulations with mean parameters are in Appendix D for comparison). As expected based on model validation (Table 1), QBM projections were more uncertain than IPM projections for all species except *P. smithiii* (Fig. 6). IPM forecasts for *P. smithiii* were very uncertain due to a very high instrinsic rate of recruitment combined with uncertainty in climate coefficients which lead to high recruitment boom years and subsequent busts when young plants suffer high mortality (Appendx C). When we included model error and parameter uncertainty, forecast changes in proportional cover always spanned a wide range of negative to positive values. In other words, neither model could predict whether a climate perturbation would increase or decrease equilibrium population size.

Discussion

Population models built using individual-level data allow inference on demographic processes, but they can only forecast future population states across the (typically limited) spatial extent of the observations. Population-level data are much easier to collect across broad spatial extents, so models built using such data offer an appealing alternative to traditional population models (Queenborough et al. 2011). However, density-structured

18

models rely on the aggregation of individual-level data. This creates a potential problem if such models are to be used in a climate change context because it is individuals, not populations, which respond to climate (Clark et al. 2012). Are models based on population-level metrics as sensitive to climate as models based on individual-level metrics? Do these two types of models produce consistent forecasts? Do we need detailed demographic data to forecast the impacts of climate change?

The importance of demographic data

Our comparison of a traditional, demographic population model (the IPM) with a model inspired by density-structured models (the QBM) showed that the IPM outperformed the QBM: the IPM was more accurate and precise than the QBM in out-of-sample cross validation (Table 1). The superiority of the IPM could reflect either differences in sample size or the effect of averaging over unique effects of climate on each individual-level vital rate. Although increasing sample size of quadrat percent-cover observations would be easy to do in the field, we found little evidence that it would lead to higher precision of climate coefficient estimates (Fig. 4).

We did, however, find evidence that the QBM statistical model failed to identify climate dependence for some vital rates (Fig. 5). For no species were climate effects from the QBM strongly correlated with all three vital rates (Fig. 5). Freckleton et al. (2011) acknowledge that averaging over complex stage dependence will lead to poorly specified models. This is analagous to our situation, but instead of averaging over complex life histories, we are averaging over complex climate dependence. Though our work here focused on plant species, this finding is applicable to any species with vital rates that respond uniquely to weather/climate.

Our interpretation is that the QBM is "missing" climate signals associated with at least one vital rate for each species. This leads to inaccurate and imprecise forecasts because

19

the QBM statistical model struggles to explain variation due to climate variables that have positive and negative impacts on different vital rates. When this is the case, as it is for all our species to varying degrees (Fig. 3), forecasts from models based on population-level data will fail. Our result is consistent with related work on the importance of individual-level data to forecast population responses to exogenous drivers (Clark et al. 2011a, 2011b, 2012, Galván et al. 2014).

Detailed demographic data appears to be necessary to forecast climate change impacts on plant populations when vital rates have unique climate responses. How then can we build models to make forecasts for the landscape and regional scales beyond the scope of traditional population models (Queenborough et al. 2011)? There are alternatives to density-structured models. For example, Clark et al. (2011a) use Forest Inventory and Analysis (FIA) data to parameterize a population model with multiple vital rates and climate dependence. Distributed efforts such as PlantPopNet (http://plantago.plantpopnet.com) will allow researchers to estimate variation around climate responses for widespread species by taking advantage of spatial variation in climate (e.g. Doak and Morris 2010). Finally, new approaches on the horizon that leverage photo/video of plots and advanced object recognition algorithms (e.g. Liu et al. 2014) will increase the efficiency of plant mapping and digitizing efforts.

The challenge of uncertainty

An important, but unexpected, result of our analysis was the great uncertainty in forecasts, even for our best model. The typical approach in ecology is to use point estimates of model parameters to project populations forward according to the specified model, usually allowing for some variability around the determinstic process (e.g. Battin et al. 2007, Jenouvrier et al. 2009, Adler et al. 2012). If we follow tradition and calculate the mean response to climate perturbation with only model error and interannual variation included,

20

the IPM and the QBM produce opposing forecasts for three of four species (Fig. D1). It would be tempting to interpret this inconsistency as further evidence for the superiority of the IPM. However, if we introduce parameter uncertainty, the forecasts are actually indistinguishable (Fig. 6), though the IPM projections are generally more precise (consistent with our cross-validation results). The real story is that both models produce highly uncertain forecasts. For all species, the 90% quantiles of predicted changes in population size overlapped zero; we cannot even predict whether a change in precipitation or temperature will cause populations to increase or decrease. This result held when we tried perturbing climate by 10% and 20% as well.

Our results highlight the state of affairs in ecology when it comes to forecasting the impacts of climate change. The analysis we conducted here could be considered at the forefront of ecological forecasting with respect to the statistical approach employed (hierarchical Bayesian), the type of population model we used (density-dependent, stochastic IPM with parameter uncertainty), and the amount of high quality data we had at our disposal (14 years of individual-level data). Yet, model predictions proved so uncertain that any forecast, when bounded with model and parameter uncertainty, would be uninformative.

How might we improve on this state of affairs? First, forecasts could be improved by matching the spatial scale of predictor variables with the spatial scale of observations. One of the major limitations of the models we fit here is that the climate data are collected at a larger scale than the individual-level observations of plant size. Climate covariates only vary by year, with no spatial variability within years. Thus, even if we fit models to individual-level data, we are missing the key interaction point between weather and individual plants (Clark et al. 2011b) because all observations share the same climate covariates. Demographic studies should be designed with at least plot-level measurements of climate related variables (e.g., soil moisture). Second, accurately detecting climate signals will take even longer time series. Recent theoretical work on detecting climate signals in noisy data suggests that even advanced approaches to parameter fitting require 20-25 year

21

time series (Teller et al. 2016). Third, ecologists need a stronger commitment to reporting uncertainty. Although most modeling studies explicitly consider model uncertainty, parameter uncertainty is often ignored. In some cases this is because the most convenient statistical methods make it difficult to propogate parameter uncertainty. Yet even Bayesian approaches that allow integration of model fitting and forecasting (Hobbs and Hooten 2015) are not simple when using modeling approaches like integral projection models that separate the model fitting and simulation stages (Rees and Ellner 2009). However, as we have done here, it is still possible to include parameter uncertainty by drawing parameter values from MCMC iterations, taking care to draw all parameters from the same chain and iteration to account for their correlations. Only by being honest about our forecasts can we begin to produce better ones, and forecasts reported without parameter error are disingenuous. Ignoring parameter error may be justifiable when the goal is investigating basic processes, but it is indefensible when forecasting is the goal.

Conclusions

This work is not a critique of density-structured population models. We are confident that density-structured models will prove to be a valuable tool for many applications. However, our analysis represents the first comparison, to our knowledge, of population models based on individual and aggregated forms of the same data in a climate change context. Our results confirm theoretical arguments (Clark et al. 2011b) and empirical evidence (Clark et al. 2011a, 2012) that individual responses are critical for predicting species' responses to climate change. It seems there is no short cut to producing accurate and precise population forecasts: we need detailed demographic data to forecast the impacts of climate change on populations. Given the importance of demographic data and its current collection cost, we need modern methods to collect demographic data more efficiently across environmental gradients in space and time.

22

Our results also offer a cautionary tale because forecast uncertainty was large for both model types. Even with 14 years of detailed demographic data and sophisticated modeling techniques, our projections contained too much uncertainty to be informative. Uncertainty in demographic responses to climate can be reduced by collecting (1) longer time series and (2) climate covariates that match the scale of inference (e.g., plot rather than landscape level climate/weather metrics).

Acknowledgments

Tables

Table 1: Accuracy (mean absolute error, MAE) and precision (90% Distance) of out of sample predictions. Forecasts were made without random year effects; only climate covariates could explain year-to-year variation. 90% Distance refers to the average distance between the upper and lower 90th percentiles of the 100 predicted values for each quadrat-year combination.

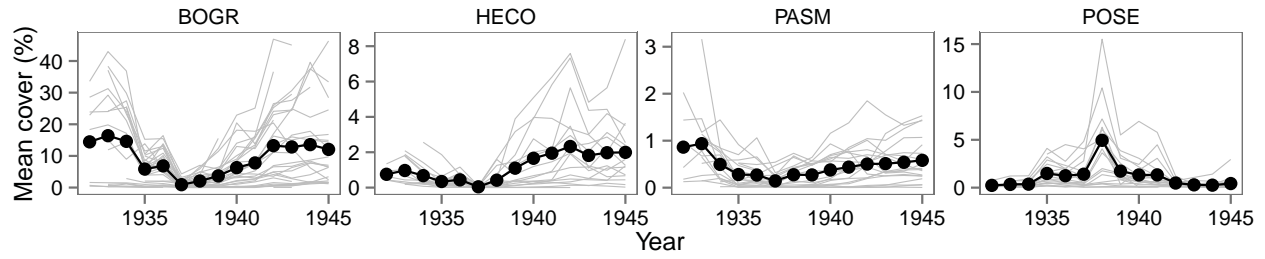| Species	Model	MAE	90% Distance	Mean Obs. Cover
BOGR	IPM	4.61	22.41	8.26
BOGR	QBM	4.06	29.18	8.26
HECO	IPM	0.59	1.93	1.22
HECO	QBM	0.60	5.64	1.22
PASM	IPM	0.15	0.49	0.40
PASM	QBM	0.20	1.59	0.40
POSE	IPM	0.71	1.66	1.23
POSE	QBM	0.76	3.52	1.23

Figures

Figure 1: Time series of average percent cover over all quadrats for our four focal species: *Bouteloua gracilis* (BOGR), *Hesperostipa comata* (HECO), *Pascopyrum smithii* (PASM), and *Poa secunda* (POSE). Light grey lines show trajectories of individual quadrats. Note the different y-axis scales across panels.
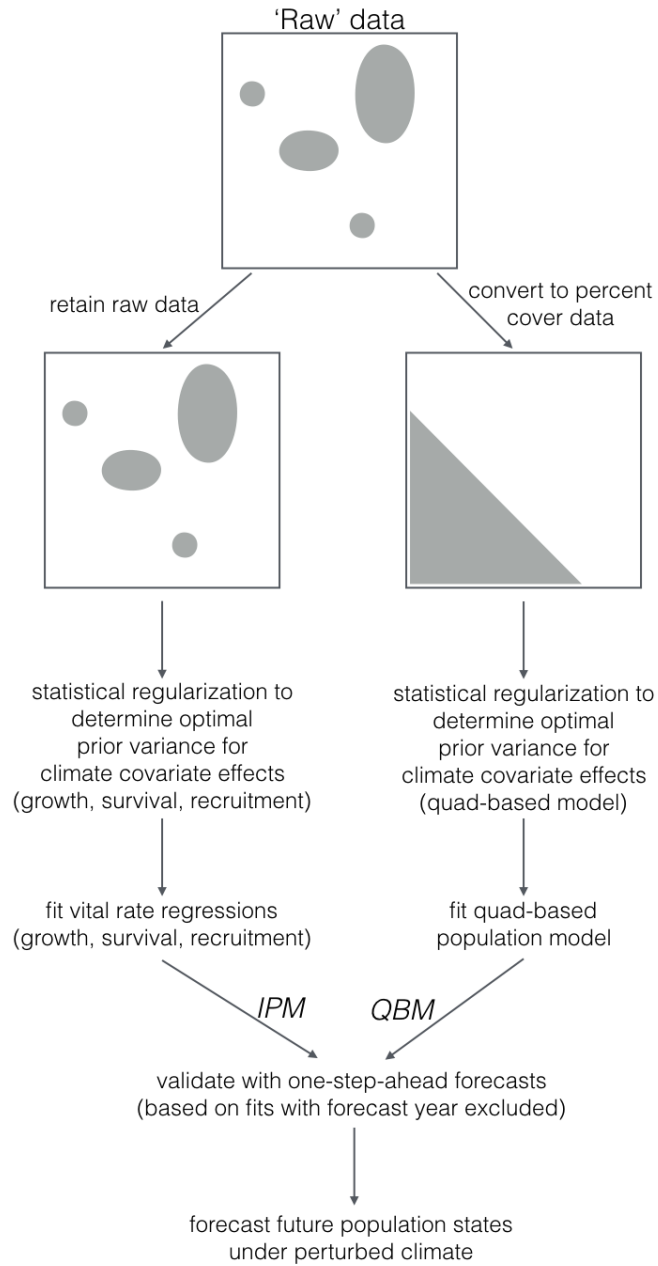
'Raw' data

retain raw data

convert to percent
cover data

statistical regularization to
determine optimal
prior variance for
climate covariate effects
(growth, survival, recruitment)

statistical regularization to
determine optimal
prior variance for
climate covariate effects
(quad-based model)

fit vital rate regressions
(growth, survival, recruitment)

fit quad-based
population model

IPM   QBM

validate with one-step-ahead forecasts
(based on fits with forecast year excluded)

forecast future population states
under perturbed climate

Figure 2: Work flow of the data aggregation, model fitting, and population simulating.
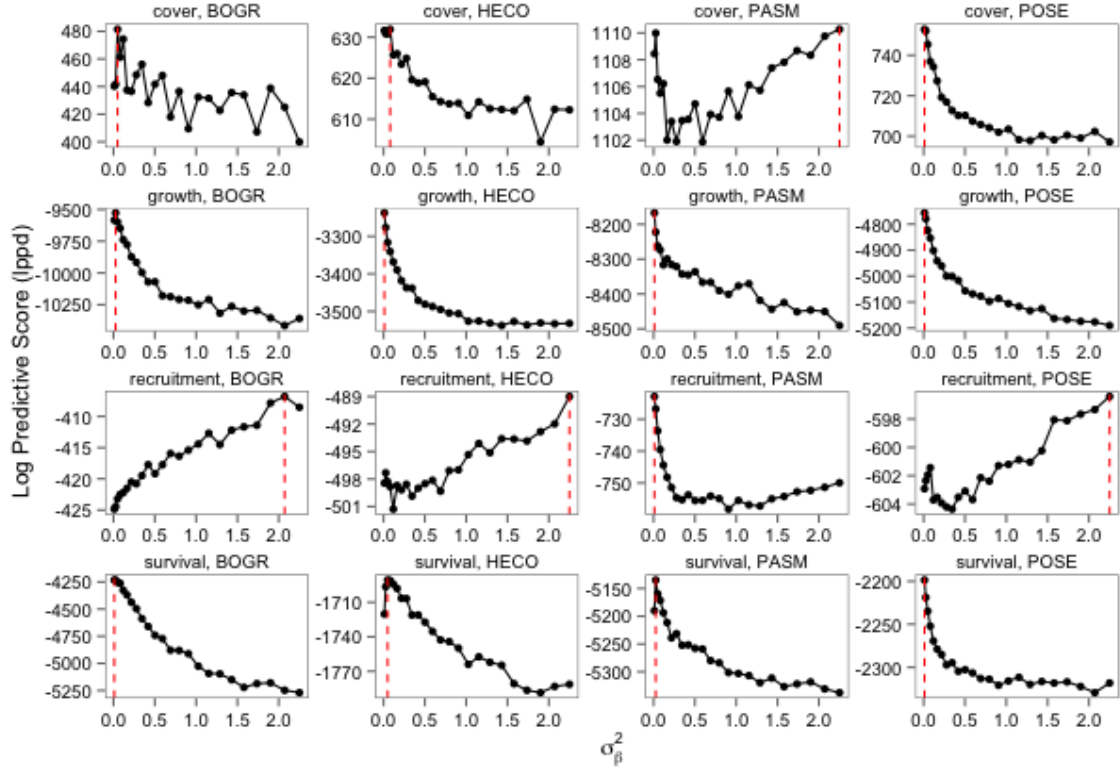
Figure 3: Cross validation scores (summed log pointwise predictive density) plotted against the prior variance for $\boldsymbol{\beta}_C$. The optimal score for prediction for each species-vital rate combination is shown with a vertical red line.
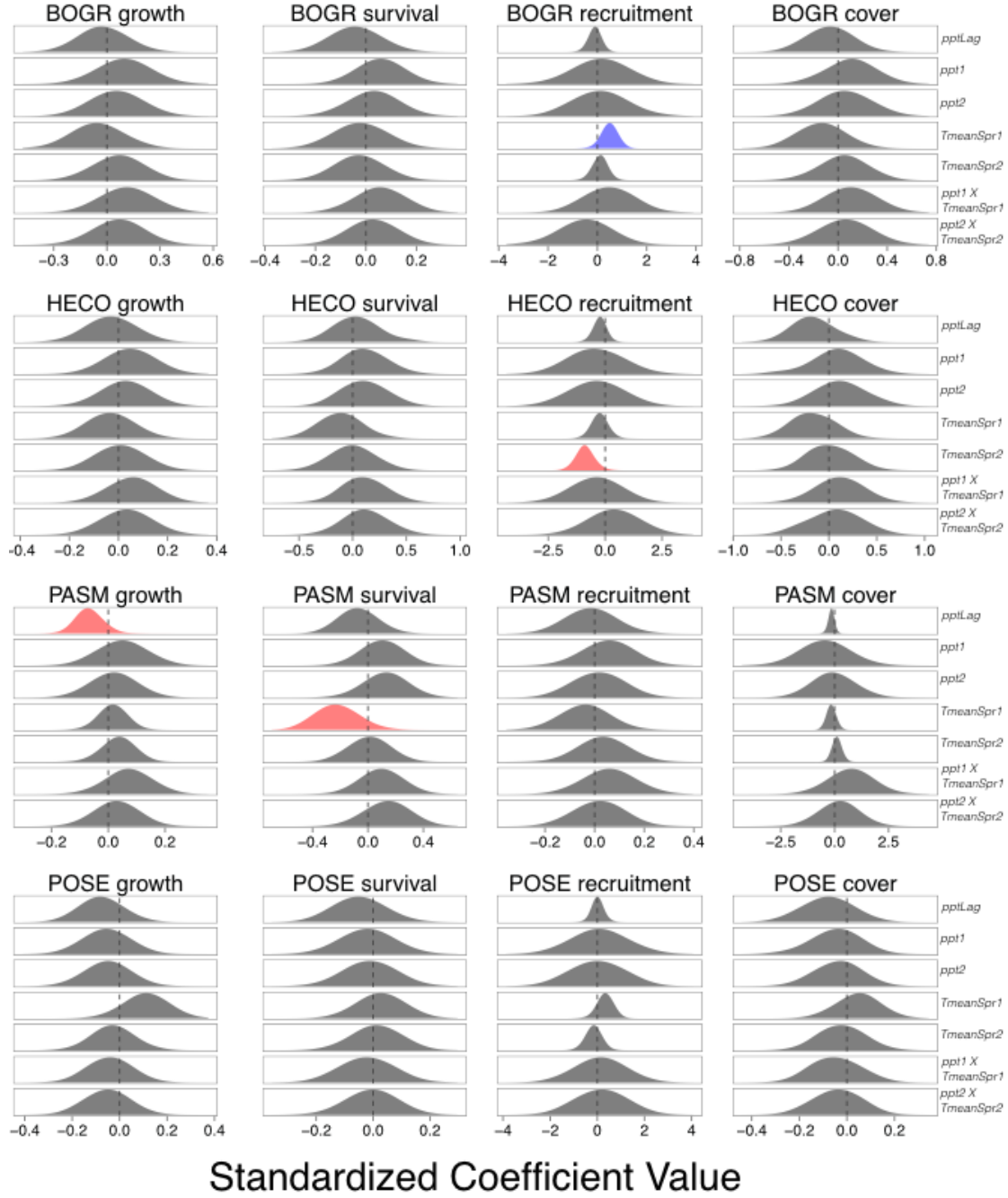
Figure 4: Posterior distributions of climate effects ($\boldsymbol{\beta}_C$) for each species and vital rate statistical model. Since our priors were constrained via ridge-regression, we highlight climate effects whose 80% credible intervals do not overlap zero (red for negative coefficients, blue for positive coefficients). Kernel bandwidths of posterior densities were adjusted by a factor of 4 for visual clarity.
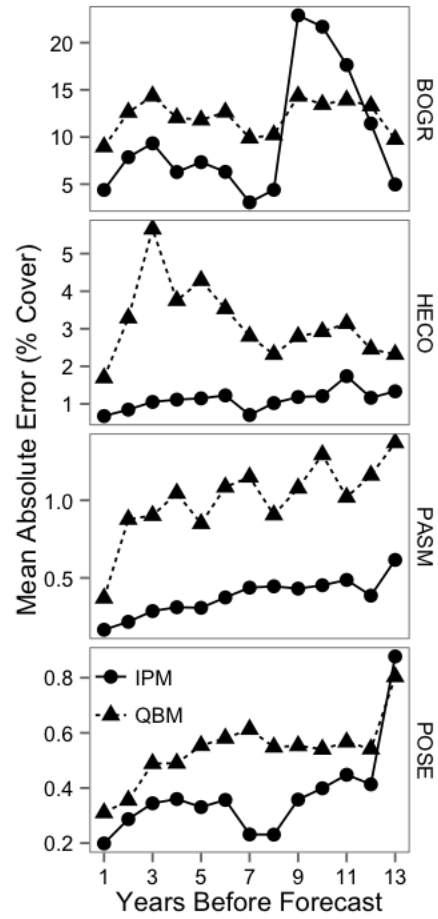
Figure 5: The forecast horizons for both models when used to forecast the final observation (cover in year 1945) starting from all possible prior years. For example, simulations initialized with cover in 1932 have 13 years before the forecast.
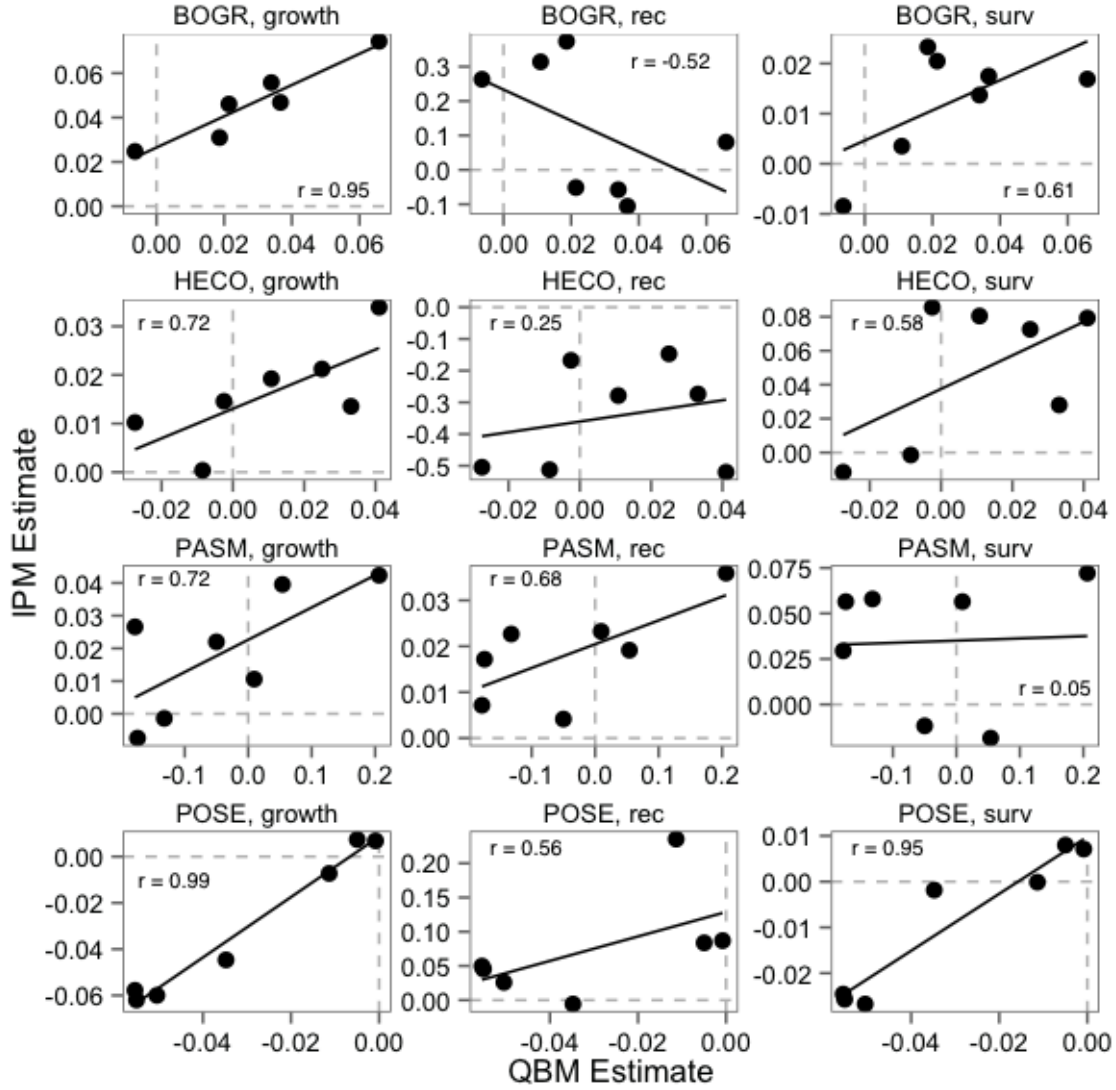
Figure 6: Correlations between QBM and IPM estimates of climate effects. We ignore sizeXclimate interactions since these are not directly comparable across model types. The QBM does not have multiple vital rates, so its values are repeated across panels within each species. Across top panels, 'growth' = growth regression, 'rec' = recruitment regression, 'surv' = survival regression.
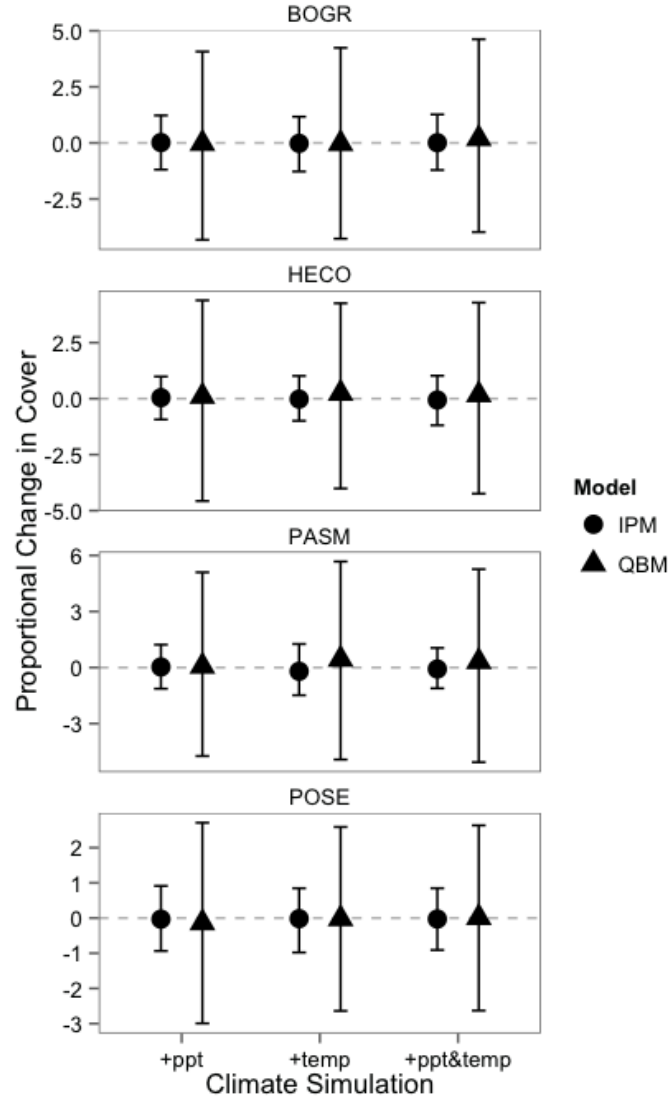
Figure 7: Mean (points) and 90% quantiles (errorbars) for the proportional difference between baseline simulations (using observed climate) and the climate pertubation simulation on the x-axis. We calculated proportional difference as log(perturbed climate cover) - log(observed climate cover), where 'perturbed' and 'observed' refer to the climate time series used to drive interannual variation in the simulations. Model error and parameter uncertainty were propagated through the simulation phase.

References

Adler, P. B., H. J. Dalgleish, and S. P. Ellner. 2012. Forecasting plant community impacts of climate variability and change: when do competitive interactions matter? Journal of Ecology 100:478–487.

Adler, P. B., S. P. Ellner, and J. M. Levine. 2010. Coexistence of perennial plants: An embarrassment of niches. Ecology Letters 13:1019–1029.

Anderson, J., L. Vermeire, and P. B. Adler. 2011. Fourteen years of mapped, permanent quadrats in a northern mixed prairie, USA. Ecology 92:1703.

Araújo, M. B., and A. T. Peterson. 2012. Uses and misuses of bioclimatic envelope modeling. Ecology 93:1527–1539.

Battin, J., M. W. Wiley, M. H. Ruckelshaus, R. N. Palmer, E. Korb, K. K. Bartz, and H. Imaki. 2007. Projected impacts of climate change on salmon habitat restoration. Proceedings of the National Academy of Sciences of the United States of America 104:6720–6725.

Chu, C., and P. B. Adler. 2014. When should plant population models include age structure? Journal of Ecology 102:531–543.

Chu, C., and P. B. Adler. 2015. Large niche differences emerge at the recruitment stage to stabilize grassland coexistence. Ecological Monographs 85:373–392.

Chu, C., K. M. Havstad, N. Kaplan, W. K. Lauenroth, M. P. McClaran, D. P. Peters, L. T. Vermeire, and P. B. Adler. 2014. Life form influences survivorship patterns for 109 herbaceous perennials from six semi-arid ecosystems. Journal of Vegetation Science 25:947–954.

Clark, J. S., and O. N. Bjørnstad. 2004. Population time series: Process variability, observation errors, missing values, lags, and hidden states. Ecology 85:3140–3150.

Clark, J. S., D. M. Bell, M. H. Hersh, and L. Nichols. 2011a. Climate change vulnerability of forest biodiversity: Climate and competition tracking of demographic rates. Global Change Biology 17:1834–1849.

Clark, J. S., D. M. Bell, M. H. Hersh, M. C. Kwit, E. Moran, C. Salk, A. Stine, D. Valle, and K. Zhu. 2011b. Individual-scale variation, species-scale differences: Inference needed to understand diversity.

Clark, J. S., D. M. Bell, M. Kwit, A. Stine, B. Vierra, and K. Zhu. 2012. Individual-scale inference to anticipate climate-change vulnerability of biodiversity. Philosophical Transactions of the Royal Society B: Biological Sciences 367:236–246.

Clark, J. S., D. Bell, C. Chu, B. Courbaud, M. Dietze, M. Hersh, J. HilleRisLambers, I. Ibáñez, S. LaDeau, S. McMahon, J. Metcalf, J. Mohan, E. Moran, L. Pangle, S. Pearson, C. Salk, Z. Shen, D. Valle, and P. Wyckoff. 2010. High-dimensional coexistence based on individual variation: a synthesis of evidence. Ecological Monographs 80:569–608.

Clark, J. S., S. R. Carpenter, M. Barber, S. Collins, A. Dobson, J. A. Foley, D. M. Lodge, M. Pascual, R. Pielke, W. Pizer, C. Pringle, W. V. Reid, K. A. Rose, O. Sala, W. H.

Schlesinger, D. H. Wall, and D. Wear. 2001. Ecological forecasts: an emerging imperative. Science (New York, N.Y.) 293:657–660.

Clark, J. S., A. E. Gelfand, C. W. Woodall, and K. Zhu. 2014. More than the sum of the parts: Forest climate response from joint species distribution models. Ecological Applications 24:990–999.

Dalgleish, H. J., D. N. Koons, M. B. Hooten, C. A. Moffet, and P. B. Adler. 2011. Climate influences the demography of three dominant sagebrush steppe plants. Ecology 92:75–85.

Doak, D. F., and W. F. Morris. 2010. Demographic compensation and tipping points in climate-induced range shifts. Nature 467:959–962.

Elith, J., and J. R. Leathwick. 2009. Species Distribution Models: Ecological Explanation and Prediction Across Space and Time.

Ellner, S. P., and M. Rees. 2006. Integral projection models for species with complex demography. The American naturalist 167:410–428.

Freckleton, R. P., W. J. Sutherland, A. R. Watkinson, and S. A. Queenborough. 2011. Density-structured models for plant population dynamics. American Naturalist 177:1–17.

Galván, J. D., J. J. Camarero, and E. Gutiérrez. 2014. Seeing the trees for the forest: Drivers of individual growth responses to climate in Pinus uncinata mountain forests. Journal of Ecology 102:1244–1257.

Guisan, A., and W. Thuiller. 2005. Predicting species distribution: Offering more than simple habitat models.

Hobbs, N. T., and M. B. Hooten. 2015. Bayesian Models: A Statistical Primer for Ecologists. Princeton University Press, Princeton.

Hooten, M. B., and N. T. Hobbs. 2015. A guide to Bayesian model selection for ecologists. Ecological Monographs 85:3–28.

Jenouvrier, S., H. Caswell, C. Barbraud, M. Holland, J. Stroeve, and H. Weimerskirch. 2009. Demographic models and IPCC climate projections predict the decline of an emperor penguin population. Proceedings of the National Academy of Sciences of the United States of America 106:1844–1847.

Lauenroth, W. K., and P. B. Adler. 2008. Demography of perennial grassland plants: Survival, life expectancy and life span. Journal of Ecology 96:1023–1032.

Liu, Y., Y. Jang, W. Woo, and T.-K. Kim. 2014. Video-Based Object Recognition Using Novel Set-of-Sets Representations.

Luo, Y., K. Ogle, C. Tucker, S. Fei, C. Gao, S. LaDeau, J. S. Clark, and D. S. Schimel. 2011. Ecological forecasting and data assimilation in a data-rich era. Ecological Applications 21:1429–1442.

Maiorano, L., R. Cheddadi, N. E. Zimmermann, L. Pellissier, B. Petitpierre, J. Pottier, H. Laborde, B. I. Hurdu, P. B. Pearman, A. Psomas, J. S. Singarayer, O. Broennimann, P. Vittoz, A. Dubuis, M. E. Edwards, H. A. Binney, and A. Guisan. 2013. Building the niche

through time: using 13,000 years of data to predict the effects of climate change on three tree species in Europe. Global Ecology and Biogeography 22:302–317.

Merow, C., A. M. Latimer, A. M. Wilson, S. M. McMahon, A. G. Rebelo, and J. A. Silander. 2014. On using integral projection models to generate demographically driven predictions of species' distributions: development and validation using sparse data. Ecography 37:1167–1183.

Pearson, R. G., and T. P. Dawson. 2003. Predicting the impacts of climate change on the distribution of species: Are bioclimate envelope models useful? Global Ecology and Biogeography 12:361–371.

Perretti, C. T., S. B. Munch, and G. Sugihara. 2013. Model-free forecasting outperforms the correct mechanistic model for simulated and experimental data. Proceedings of the National Academy of Sciences of the United States of America 110:5253–5257.

Petchey, O. L., M. Pontarp, T. M. Massie, S. Kéfi, A. Ozgul, M. Weilenmann, G. M. Palamara, F. Altermatt, B. Matthews, J. M. Levine, D. Z. Childs, B. J. McGill, M. E. Schaepman, B. Schmid, P. Spaak, A. P. Beckerman, F. Pennekamp, and I. S. Pearse. 2015. The ecological forecast horizon, and examples of its uses and determinants. Ecology Letters 18:597–611.

Piantadosi, S., D. P. Byar, and S. B. Green. 1988. The Ecological Fallacy. American Journal of Epidemiology 127:893–904.

Queenborough, S. A., K. M. Burnet, W. J. Sutherland, A. R. Watkinson, and R. P. Freckleton. 2011. From meso- to macroscale population dynamics: A new density-structured approach. Methods in Ecology and Evolution 2:289–302.

R Core Team. 2013. R: A language and environment for statistical computing.

Rees, M., and S. P. Ellner. 2009. Integral projection models for populations in temporally varying environments. Ecological Monographs 79:575–594.

Schurr, F. M., J. Pagel, J. S. Cabral, J. Groeneveld, O. Bykova, R. B. O'Hara, F. Hartig, W. D. Kissling, H. P. Linder, G. F. Midgley, B. Schröder, A. Singer, and N. E. Zimmermann. 2012. How to understand species' niches and range dynamics: A demographic research agenda for biogeography. Journal of Biogeography 39:2146–2162.

Stan Development Team. 2014a. Stan: A C++ Library for Probability and Sampling, Version 2.5.0.

Stan Development Team. 2014b. Rstan: the R interface to Stan, Version 2.5.0.

Sæther, B. E., S. Engen, V. Grøtan, W. Fiedler, E. Matthysen, M. E. Visser, J. Wright, A. P. Møller, F. Adriaensen, H. Van Balen, D. Balmer, M. C. Mainwaring, R. H. McCleery, M. Pampus, and W. Winkel. 2007. The extended Moran effect and large-scale synchronous fluctuations in the size of great tit and blue tit populations. Journal of Animal Ecology 76:315–325.

Taylor, C. M., and A. Hastings. 2004. Finding optimal control strategies for invasive species: a density-structured model for Spartina alterniflora. Journal of Applied Ecology 41:1049–1057.

671 Teller, B. J., P. B. Adler, C. B. Edwards, G. Hooker, R. E. Snyder, and S. P. Ellner. 2016.
672 Linking demography with drivers: climate and competition. Methods in Ecology and Evo-
673 lution 7:171–183.